International Journal of Engineering Science Invention (IJESI)
ISSN (Online): 2319 – 6734, ISSN (Print): 2319 – 6726
www.ijesi.org ||Volume 8 Issue 05 Series. IV || May 2019 || PP 11-27

Behavior of Short Reinforced Crumb Rubber Concrete Columns Subjected to Elevated Temperatures

Mohamed S. Gomaa[1], Mahmoud Elsayed[2]
[1](Lecturer, Faculty of Engineering, Fayoum University, Egypt)
[2](Lecturer, Faculty of Engineering, Fayoum University, Egypt)
Corresponding Author: Mohamed S. Gomaa

Abstract: *This paper presents experimental and numerical investigations to study the performance of heated reinforced crumbed rubber concrete short columns under axial compression load. The experimental program of this study includes testing of nine columns. The mixtures of these columns have been produced by replacing the fine aggregate with crumb rubber at designated replacement levels of zero, 10%, and 20% by total fine aggregate volume. Three columns have been kept as control columns, while the other six columns have been exposed to elevated temperatures of 400ºC and 600 ^{o}C for a period of 3 hours. The heated columns have been left to cool down at room temperature and then axially loaded till failure. The experimental results have been utilized for validation of finite element models which have been developed using the well-known Finite Element (FE) software; ANSYS. The experimental results have shown that the percentage of loss in the residual axial capacity and the secant stiffness of columns increases as the exposure temperature increased to 400^{o}C and 600^{o}C. Increasing the rubber amount led to a decrease in the strength and the stiffness magnitudes. Nevertheless, the ductility was significantly improved by using crumb rubber. Furthermore, the constructed FE models have succeeded in simulating the temperature distribution across the column's cross section and in predicting its ultimate axial load capacity.*

Keywords –*Crumb rubber, Reinforced Concrete, Short Columns, Temperature.*

Date of Submission: 20-05-2019 Date of acceptance: 03-06-2019

I. INTRODUCTION

Concrete is one of the most widely used materials in the world and due to massive leap in concrete structures, the natural resources are depleting gradually. The availability of natural aggregates at a reasonable rate is of a big concern of the concrete industry [1]. On the other hand, due to the growing use of the automobile sector, the number of waste tires is continually increasing. Finding a useful method to dispose of waste rubber is becoming a major issue. Using recycled rubber as additives to or replacements of construction materials is a viable alternative to the disposal option [2,3]. Some researchers [4–10] studied the effects of inclusion the crumb rubber in concrete on the physical, thermal and mechanical properties of the concrete. It was found that the use of rubber reduces the compressive strength of the concrete to a certain extent. Bisht and Ramana [11] proved that increasing the rubber content up to 4%, the compressive and flexural strengths examine slight decrease and water absorption and abrasion resistance are also marginally affected. Al-Tayeb et al. [12] and Dong et al. [13] reported that the compressive strength decreased by increasing the percentage of crumb rubber content. Liuet al. [14] investigated the influence of the percentage of recycled rubber on the performances of concrete. It was observed that increasing the volume fractions of rubber particles led to improve the durability and show an adverse effect on the mechanical strength. Atahan A. O., and Yücel A. [15] reported that increasing the amount of rubber in concrete led to a decrease in the compressive strength and modulus values, while it increases concrete's impact resistance and energy dissipation capacity. Abended et al [16] carried out an experimental test to study the behavior of concrete-filled steel tubes (CFST) incorporating rubberized concrete. Their test results indicated that the use of rubber crumb improved the fresh-state workability but it had an adverse influence on the compressive strength of the concrete. Youssf et al [17] provide different mechanical properties of FRP confined and unconfined CRC with different concrete mixtures having 0%, 10%, 20%, 30%, 40%, and 50% rubber volume replacement of fine aggregate. Mendis et al [18] carried out experimental and numerical studies to investigate the flexural shear behavior of reinforced crumbed rubber concrete beams with different volumes of rubber, and with or without shear reinforcement. The compressive strength behavior of rubber crumb and steel fiber reinforced recycled aggregate concrete under high temperature was evaluated by Guo et al [19]. The results showed that both the compressive strength and stiffness of concrete mixes decreased after exposure to elevated temperature. Youssf et al [20] performed an experimental investigation to study the behavior of rubberized concrete columns under axial compression and incrementally increasing reverse cyclic

loading. It was observed that using crumb rubber concrete slightly improved the peak strength and reduced the ultimate drift. Yang et al [21] carried out experimental and numerical studies of rubber concrete slabs with steel reinforcement under close-in blast loading. It was found that the rubber concrete slabs with steel reinforcements are suitable structures for blast resistance.

II. EXPERIMENTAL PROGRAM

2.1. Material properties

To achieve the main goal of this study, three concrete mixtures with varying rubber contents have been prepared to be used. A concrete control mixture with zero percent of rubber and with an aimed compressive strength of 30 MPa at 28 days has been prepared. The other two mixtures have been prepared by replacing 10% and 20% of the volume of the fine aggregate with an equal volume of crumb rubber. The components of the three mixes are listed in **Table 1**. Two different types of steel reinforcements were used, Ø 6mm and Φ10 with the yield strengths of 285 MPa and 412 MPa, respectively. The used crumb rubber was fine crumb with a size which ranges between of 0.71 mm to 2.80mm; a photo for the used crumb rubber is shown in **Fig. 1.** Sieve analysis curves according to (ECP203) for all used aggregates are shown in **Fig. 2**.

Table 1: Concrete mixtures details.

Mix code	Mix proportions (Kg/m^3)			W/C	% of rubber [a]
	Cement	Fine aggregates	Coarse aggregates		
M0	360	593	1060	0.45	0
M10	360	534	1060	0.45	10
M20	360	474	1060	0.45	20

[a] By volume of the fine aggregates.

Fig. 1. Crumb rubber

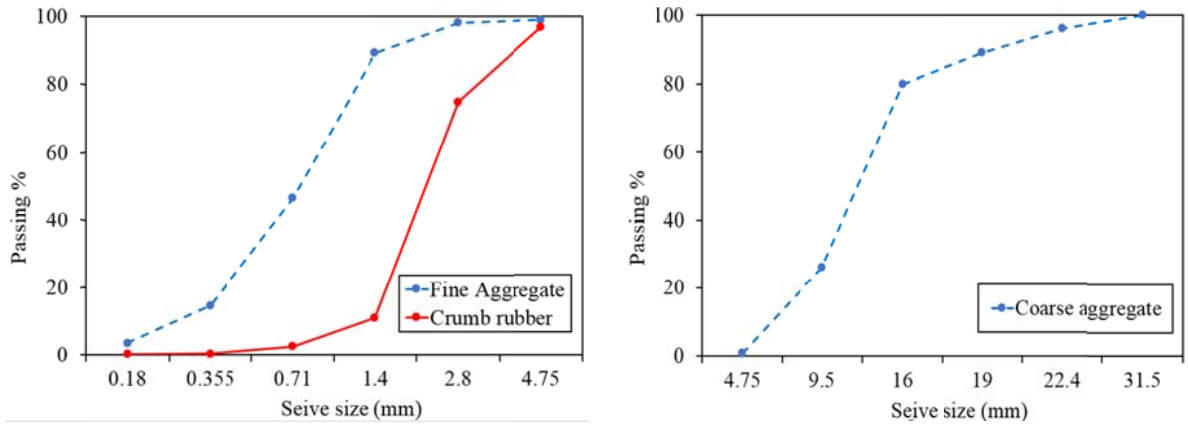

Fig. 2.Sieve analysis of the used aggregates.

2.2. Configuration of the Specimens

In order to study the performance effects of elevated temperatures on the load carrying capacity of RC square columns incorporating crumb rubber, nine RC columns have been constructed and tested experimentally. Three unheated columns have been kept as reference specimens while the remaining six columns have been exposed to elevated temperature for 3 hours, and all columns have been tested under axial compression load. All the specimens have the same square cross-section of 150 mm and a height of 1000 mm. In all columns, Ø 6mm smooth bars have been used as stirrups spaced at 100 mm at the upper and lower thirds of the columns and at 140 mm in the middle region. Furthermore, four bars of Φ10 mm diameter have been used as the longitudinal reinforcement as shown in **Fig.3**. The nine specimens have been divided into three groups [A], [B], and [C]. Each group contains three columns with 0%, 10%, and 20% rubber content replacement of the total fine aggregate volume. The specimens of group [A] have subjected to ambient temperature (unheated), while the specimens of the two other groups [B] and [C] have been heated for three hours at a temperature of 400^{o}C and 600^{o}C for group [B] and [C]; respectively. A list of the tested specimens is shown in **Table 2.**In this table, the notation "R" relates to "Room" temperature.

Table 2: Description of the test specimens

Group ID	Specimen ID [a]	Temperature
[A]	C-M0-R	Room temperature (24^{o}C)
	C-M10-R	Room temperature (24^{o}C)
	C-M20-R	Room temperature (24^{o}C)
[B]	C-M0-400	400^{o}C - for a duration of 3 hours
	C-M10-400	400^{o}C - for a duration of 3 hours
	C-M20-400	400^{o}C - for a duration of 3 hours
[C]	C-M0-600	600^{o}C - for a duration of 3 hours
	C-M10-600	600^{o}C - for a duration of 3 hours
	C-M20-600	600^{o}C - for a duration of 3 hours

[a] Column - Mix code – Temperature

2.3. Heating of Columns Specimens

Heating of the tested columns to the required high temperatures has been carried out using an electric furnace of internal dimensions 400x450x1200 mm. The columns have been heated after an age of 45 days after casting them. One column with three 150 mm cubes were placed in the furnace and heated for a period of 3 hours at the required temperature, as shown in **Fig. 4**. After reaching the required temperature for the planed duration, the furnace has been switched off and the specimens have been allowed to cool off naturally to the room temperature by opening the furnace door. **Fig. 5** shows the time-temperature curves for the heated columns. From the figure it can be noted that, the higher the crumb rubber content is, the lower the gradient of the temperature inside the center of the column is. A possible explanation for this is that, using the crumb rubber results in decreasing the voids in the micro-structure of the concrete mixture which, in turn, resulted in decreasing its porosity and have a significant influence on its behavior. The porosity of concrete depends on several factors related to the water-cement ratio and the level of internal micro-cracking. During heating, the porosity of concrete is increased due to water evaporation.

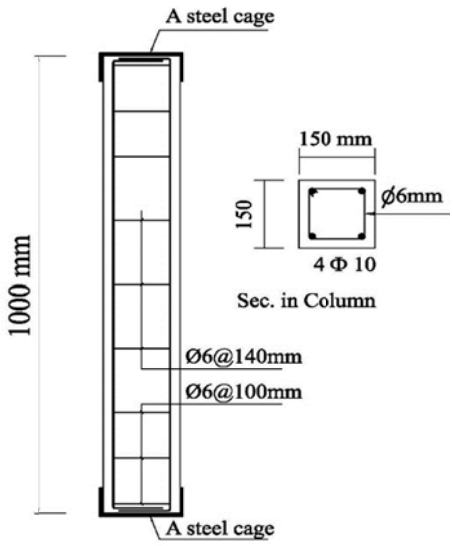

Fig. 3. Columns designations, dimensions and reinforcement arrangement.

Fig. 4. Column inside the electric furnace ready for heating.

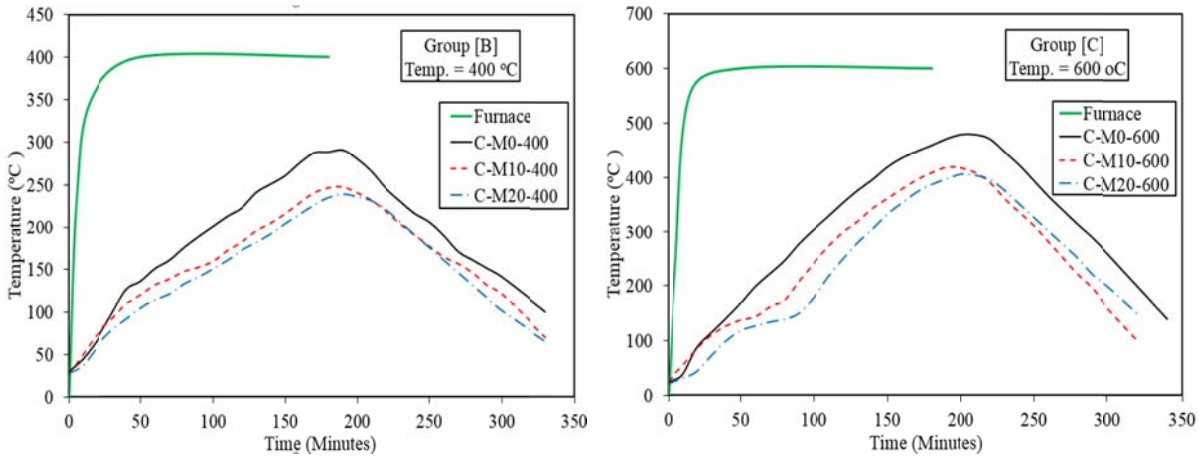

Fig. 5 Time–temperature curves during column heating for groups [B] and [C].

III. EXPERIMENTAL RESULTS

The effects of crumb rubber content and elevated temperature on the behavior of RCRC short columns, including the compressive strength, ultimate axial load capacity, and secant stiffness have been obtained.

3.1 Compressive Strength

The compressive strengths of each concrete mix, including both heated and unheated specimens are shown in **Table 3**. According to this table, it can be noticed that for the unheated concrete specimens, increasing the rubber content from 10% to 20% of the volume of fine aggregate leads to a decrease in the compressive strength from 72% of the compressive strength of the original case where no crumb rubber for the M10 mix (10% crumb rubber) to 61% for the M20 mix (20% crumb rubber). Besides, the compressive strength has generally decreased with the increase of the exposure to elevated temperatures. Furthermore, about 61% and 50 % of the compressive strength of the post heated concrete have been retained after heating to 400 ºC for the 10% and 20% crumb rubber; respectively. While, after heating to 600 ºC these values have further reduced to 4% and 36 % for the 10% and 20% crumb rubber; respectively.

A comparison of the results shows that the inclusion of rubber generally reduces the rate of loss of the concrete strength and this trend is clearer in the case of the elevated temperatures. This is may be owing to the existence of rubber, as it leaves space for water vapor to escape and helps to release the pore pressure and thus reduces its damage on the concrete structure Li et al [22].

Fig. 6. Experimental test set up

Table 3: The results of compressive strength

Mix code	compressive strength (MPa)			% residual in compressive strength with respect to C-M0-R		
	24ºC	400ºC	600ºC	24ºC	400ºC	600ºC
M0	36	26	22	0.00	72.22	61.11
M10	29	22	17	86.11	61.11	47.22
M20	25.5	18	13	70.83	50.00	36.11

3.1.1 Test observations and failure mode

The surfaces of the columns have been carefully observed after the heating process. Although spalling was not the main parameter to be investigated in this experimental program, major explosive spalling has been occurred in some columns during heating. Random hairline cracks on the surfaces of each column and small horizontal cracks around the stirrups have been observed. As a result of the decrease of the moisture content in the concrete mix, some thermal cracks have been observed. Furthermore, it has been observed that the color of the heated columns without crumb rubber has been found to be pink, while the columns with rubber content concrete have appeared to have a more dark color as shown in **Fig. 7**. In addition, the failure modes of the tested specimens after the compression tests are shown in **Fig. 8**. As can be noticed from this figure, a typical crushing failure mode has been observed in all columns wherein the concrete at mid-height has been crushed as a result of pure axial compression. The crushing of concrete has been followed by explosive spalling. With the axial load has been increased, it has resulted in complete spalling of concrete thereby exposing the reinforcing steel bars which have been found to be bent at its mid-height. Local failure at extreme ends has been avoided as a result of providing a greater number of stirrups at the tested columns' top and bottom zones. For the heated columns that contain rubber, a less explosive failure has been noticed as the degraded concrete cover has started to spall prematurely ultimately resulting in reducing the axial capacity of the columns when the elevated temperature has been applied.

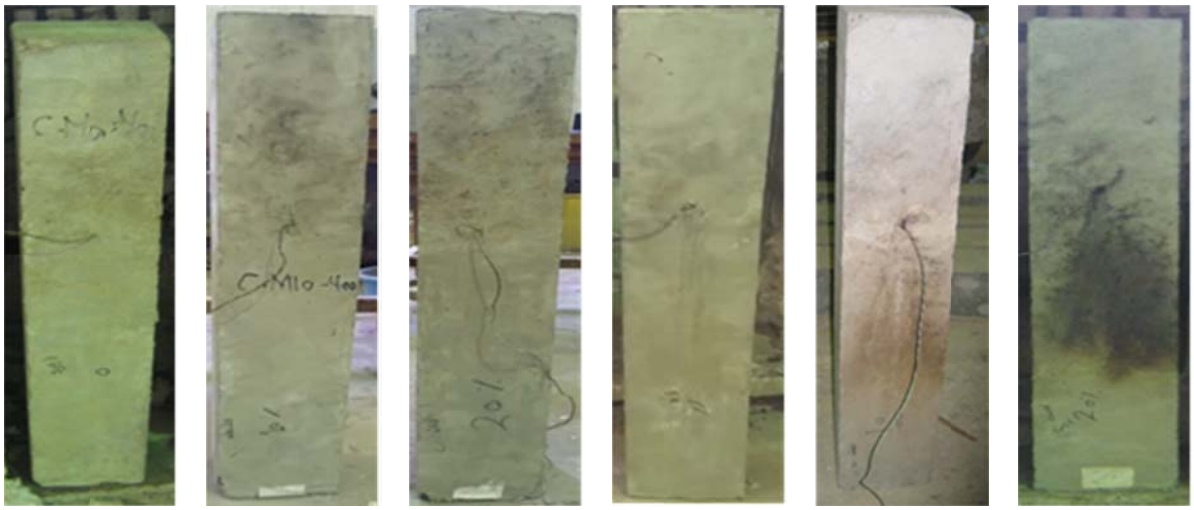

C-M0-400 C-M10-400 C-M20-400 C-M0-600 C-M10-600 C-M20-600

Fig. 7. Post heated columns of groups [B] and [C]

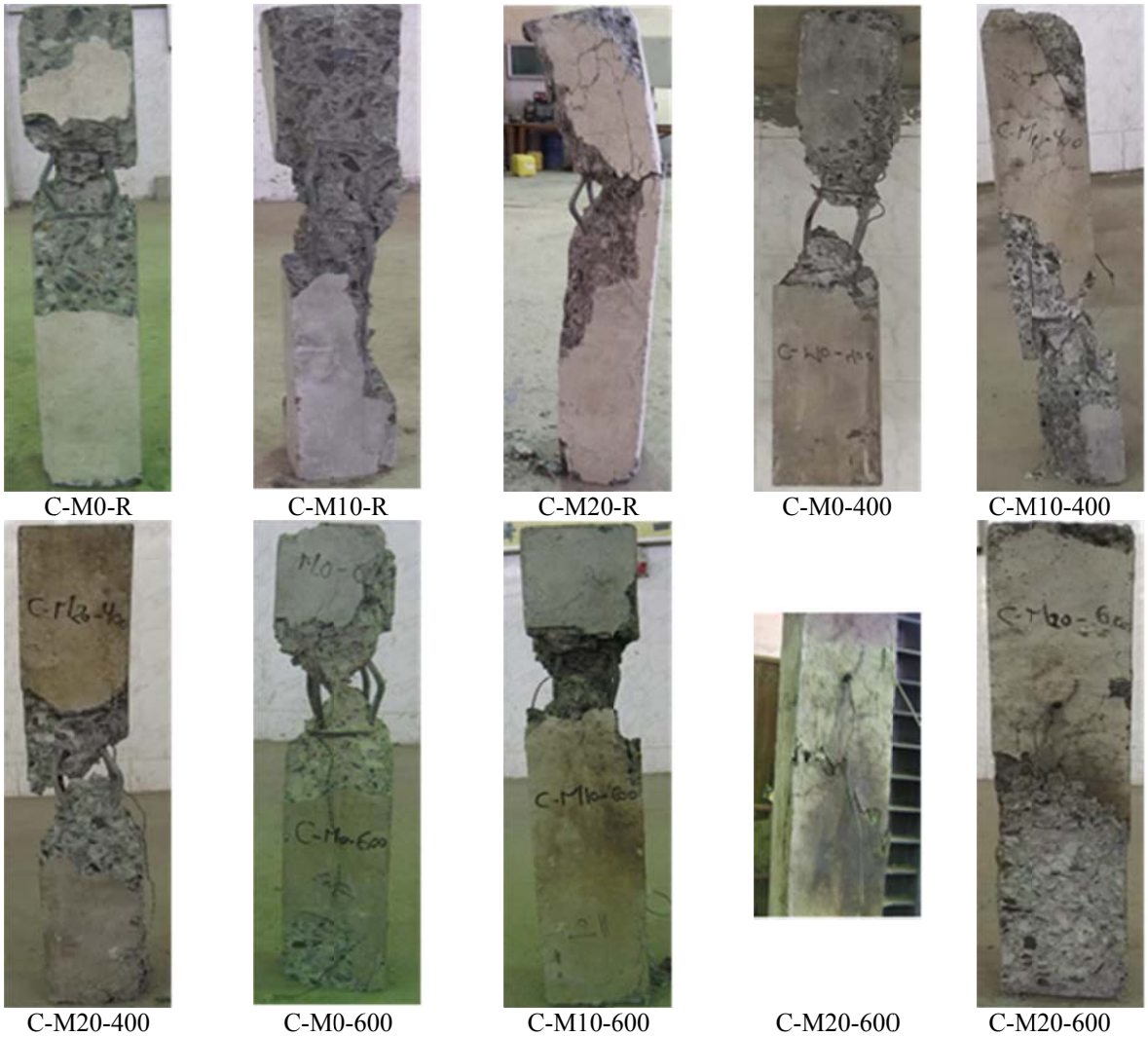

C-M0-R C-M10-R C-M20-R C-M0-400 C-M10-400

C-M20-400 C-M0-600 C-M10-600 C-M20-600 C-M20-600

Fig. 8. Cracking pattern of the tested specimens

3.1.2 Load-axial displacement behavior

The load-axial displacement relations for the tested specimens of groups [A],[B], and [C] have been obtained and are shown in **Figures 9 to 11**; respectively. The rubber content appears to have an insignificant

influence on the axial displacement at ultimate stage for the unheated columns. However, the axial displacement has apparently increased with the increase of the heating temperature. As can be observed from the figures, by increasing the temperature, the axial load carrying capacity of the column has significantly decreased. For those columns containing crumb rubber, a significant reduction in their ultimate axial capacity has been observed when subjected to elevated temperatures comparing to the corresponding control unheated columns. Furthermore, a noticeable degradation in the stiffness of the heated columns has also been noticed when the temperature has been increased. A summary of the experimental test results including the failure load and the secant stiffness of the tested specimens are listed in **Table 4**. The secant stiffness has been calculated by dividing the ultimate failure load (Pu) by the corresponding axial displacement (Δu) as schematically illustrated in **Fig. 12**.

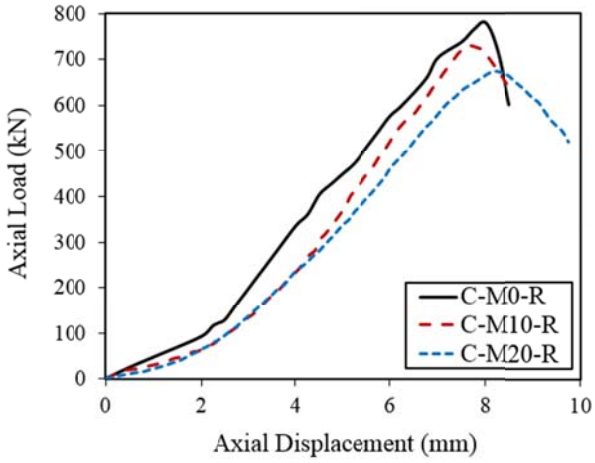

Fig. 9. Load–displacement curves for group [A]

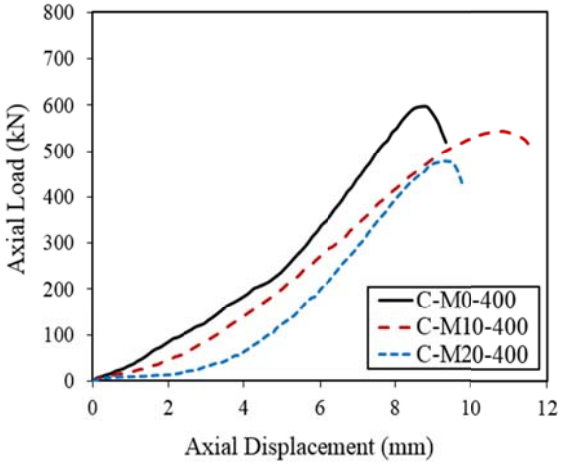

Fig. 10. Load–displacement curves for group [B]

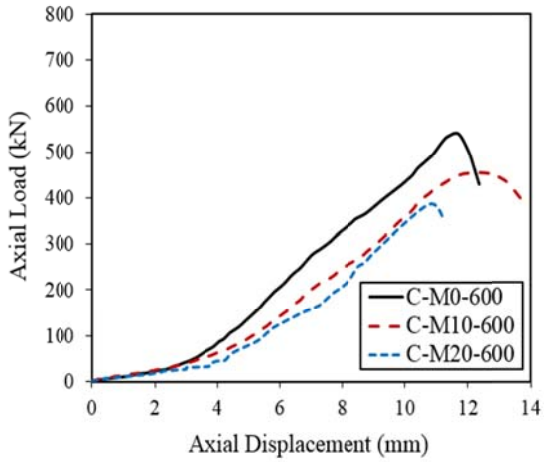

Fig. 11. Load–displacement curves for group [C]

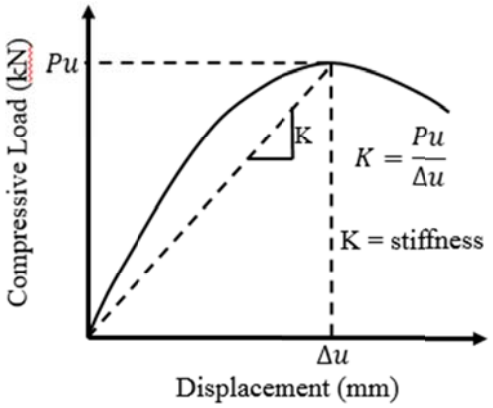

Fig. 12. Secant stiffness

According to these figures and the mentioned table, when the rubber content has been increased from 10% to 20% for the unheated columns, the loss in the axial load carrying capacity has been increased from about 7% to 14% and the percentage of loss in the secant stiffness has been increased from about 4.24% to 16.94% with respect to the control specimen (C-M0-R). In addition, and as mentioned before, the elevated temperature has a significant effect on the load carrying capacity of the columns without rubber. In this case; no crumb rubber has been used, the axial load carrying capacity of the tested columns has lost about 24% and 31% of their capacities comparing to the un-heated one when the applied elevated temperature has reached 400ºC and 600ºC; respectively.

Similar conclusions can be drawn for the columns in which the crumb rubber has been used by 10%. In this case, the columns have examined a loss in their capacities by about 26% and 38% with respect to the unheated column containing the same amount of crumb rubber when heated up to 400ºC and 600ºC; respectively. If the crumb rubber amount has reached 20% of the fine aggregate, heating the columns up to 400ºC and 600ºC has resulted in increasing the percentage of the loss in their capacities to about 32% to 43%

with respect to the unheated column containing the same amount of crumb rubber; respectively. Moreover, exposing the columns with 0%, 10%, and 20% rubber to 600^{o}C has resulted in a significant loss of their stiffness by 53%, 59%, and 63%; respectively. Generally, for both heated and unheated columns, it has been observed that the loss in their axial load capacity has been lower than the loss in their secant stiffness. This may be due to the loss in their capacity which has been accompanied; frequently, by an increase in their axial displacement.

Table 4: Summary of the test results

Group ID	Specimen ID	Failure Load (kN)	Axial displacement (mm)	Secant Stiffness	% loss with respect to C-M0-R in	
					Failure Load	Secant Stiffness
[A]	C-M0-R	788	8.00	98.50	-	-
	C-M10-R	733	8.00	91.63	6.98	4.24
	C-M20-R	675	8.25	81.82	14.34	16.94
[B]	C-M0-400	597	8.75	68.23	24.24	30.73
	C-M10-400	540	10.75	50.23	31.47	49.00
	C-M20-400	479	9.250	51.78	39.21	47.43
[C]	C-M0-600	540	11.75	45.96	31.47	53.34
	C-M10-600	455	12.50	39.57	42.26	59.83
	C-M20-600	385	10.75	35.81	51.14	63.64

IV. NUMERICAL SIMULATION USING FINITE ELEMENT (FE) METHOD

Numerical simulation usually provides a powerful tool for performing various investigations in a very small time and an extremely lower cost comparing to the experimental tests. Also, it allows carrying out comprehensive investigations and parametric studies which cannot be achieved experimentally due to lab's constraints and difficulties. In order to get trusted conclusions based on the numerical investigations, their results must be reliable and have an acceptable agreement with the experimental results. Accordingly, the main issue in the numerical investigation is how to build a numerical model that can simulate the experimental test. This process; building the numerical model, includes choosing the software which has acceptable capabilities to facilitate the modeling process, choosing the elements' types that conform with the studied problem and the required results and, the ability of applying the boundary conditions and the different types of loads in the same manner as in the experimental tests and in the real cases. If this issue is solved and the acceptable agreement between the model results and the experimental ones are achieved, then extending the study and carrying out the required investigations will be a simple task.

In this paper, our interest is to provide a numerical modeling process to get the ultimate axial capacity and to simulate the behavior of the reinforced concrete columns when subjected to elevated temperatures. Accordingly, nine numerical models have been provided for all of the tested columns using the finite element package, ANSYS. The validation of these numerical models has been obtained by comparing their numerical results with the experimental ones.

4.1 Numerical Modeling of Columns

Nine Finite Element (FE) models have been constructed using the well-known FE software; ANSYS [27], to simulate the tested columns. The 8-nodes Solid65 structural solid element, which has three degrees of freedom at each node, has been used to model the concrete. The 3-D spar 2-nodes Link8 element has been used to simulate both the longitudinal and transversal reinforcements. It is worth to mention that the Solid65 element has the ability of cracking in tension and crushing in compression to accurately model the concrete behavior at ultimate stages. The most important aspect of this element is the treatment of the nonlinear material properties, as well as, the induced plastic deformation. The shear-transfer coefficients for open and closed cracks have been set to 0.6 and 0.9; respectively. Furthermore, the Link8 element has three translational degrees of freedom at each node and it has various capabilities of creep, rotation, large deflection, and large strain.

4.2 Material Properties

As explained before in the experimental program, six of tested specimens have been subjected to elevated temperatures inside the furnace and then left to cool out to the room temperature and then the axial load test has been performed. In order to accurately simulate this process, the constituent material models have to reflect the expected changes in the materials' behavior during heating, cooling and, loading processes. To do so, the material models should be determined at specific elevated temperatures, as well as, at the room temperature. When the elevated temperature is applied to the model, the program makes linear interpolation between the

input values of the material property at different temperatures to get the required properties at the current temperature value.

At room temperature, the nonlinear material properties for the concrete with different fine aggregate types and for the reinforcing steel have been experimentally determined during the experimental program as explained before. However, at elevated temperature, the different material properties are dependent on those determined at room temperature. The relations between the material properties at elevated temperatures and those at room temperatures have been extensively investigated in many researches. Accordingly, specific relations have been selected to be used in this paper for concrete [23] and for reinforcing steel [24]. **Fig. 13** shows a schematic representation for the constitutive material models for the concrete and the reinforcing steel at elevated temperatures. It is worth to mention that for the concrete material model; the degraded part of the stress-strain relation cannot be modeled because it has a negative stiffness which is not accepted by the used software. This is to avoid the expected mathematical divergence when the negative stiffness is used. Accordingly, this part has been defined to have a zero slope instead.

Furthermore, in order to obtain the behavior of the column during heating and cooling processes, the thermal conductivity, the specific heat and, the coefficient of the thermal expansion for the concrete should be provided to the FE software to obtain the heat transfer inside the column and its effects on the column's behavior. The coefficient of the thermal expansion of concrete and reinforcing steel has been set to be 1.2×10^{-5} as per ECP203, 2007, as a constant value. On the other hand, the specific heat and the thermal conductivity of concrete are temperature dependents. Their relations with the applied temperature have been provided elsewhere [25]. **Fig. 14** shows these relations for concrete.

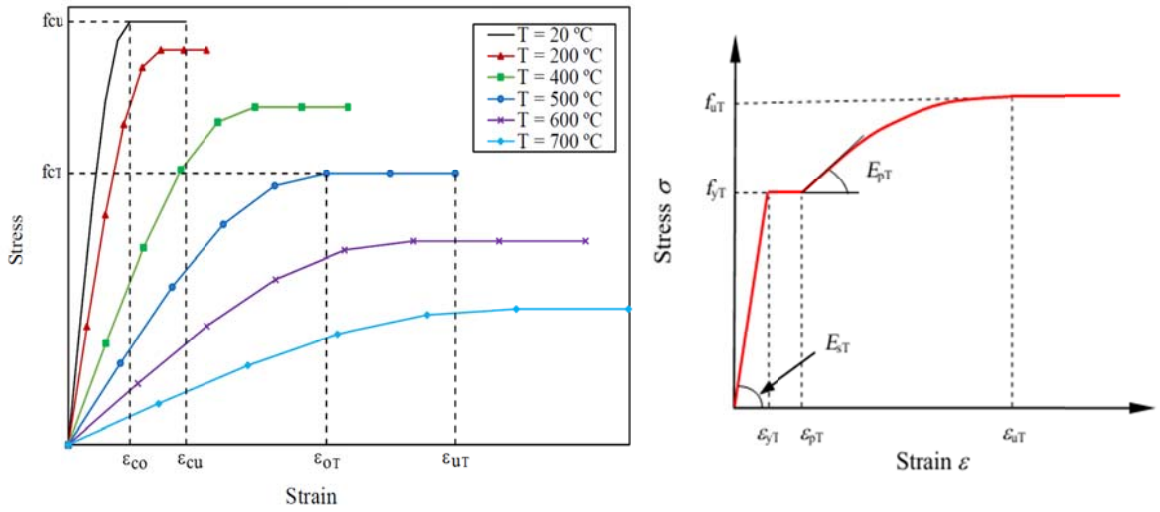

(a) Concrete (b) Reinforcing steel

Fig. 13. Schematic representation of the material models at elevated temperatures for: (a) Concrete and, (b) Reinforcing steel

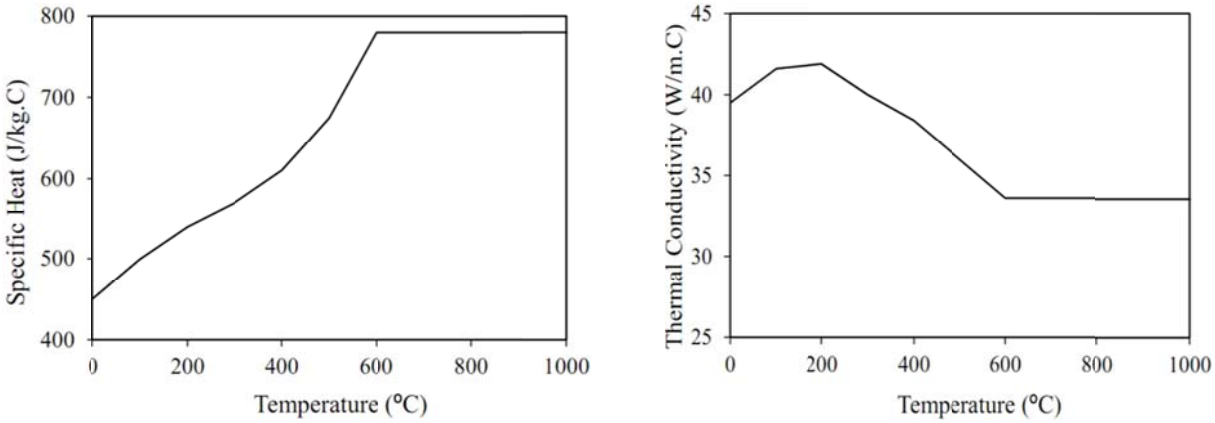

(a) Specific heat (b) Thermal conductivity

Fig. 14. Thermal properties of concrete: (a) Specific heat and (b) Thermal conductivity

4.3 Modeling and Boundary Conditions

The selected elements types; the Solid65 and the Link8 element types, have been utilized in modeling the concrete, the longitudinal reinforcement and, the transversal reinforcement of the columns along with applying the same geometrical configurations and material properties as the same as the experimental program. The mesh size has been selected to be ranged between 20mm and 27.5mm in the plane of the column cross section and between 20mm to 70mm in the height direction to locate the transversal reinforcement as in real case. The used mesh size helps in obtaining good accuracy in a reasonable solving time. The nodes at the bottom column face have been restrained from the vertical movement while the horizontal displacement has been prevented for the node at the center of the bottom face only. At the column's top face, the node which is located at the column's center has been restrained in the two orthogonal horizontal directions. This is to allow the column to expand and shrink in a free manner during heating or cooling processes which simulates the case of the column inside the furnace before applying the axial load. A 3-D view showing the column with the applied boundary conditions is shown in **Fig. 15**. In the same figure, a 2-D view that illustrates the longitudinal and the transversal reinforcement of the column is also shown in the same figure.

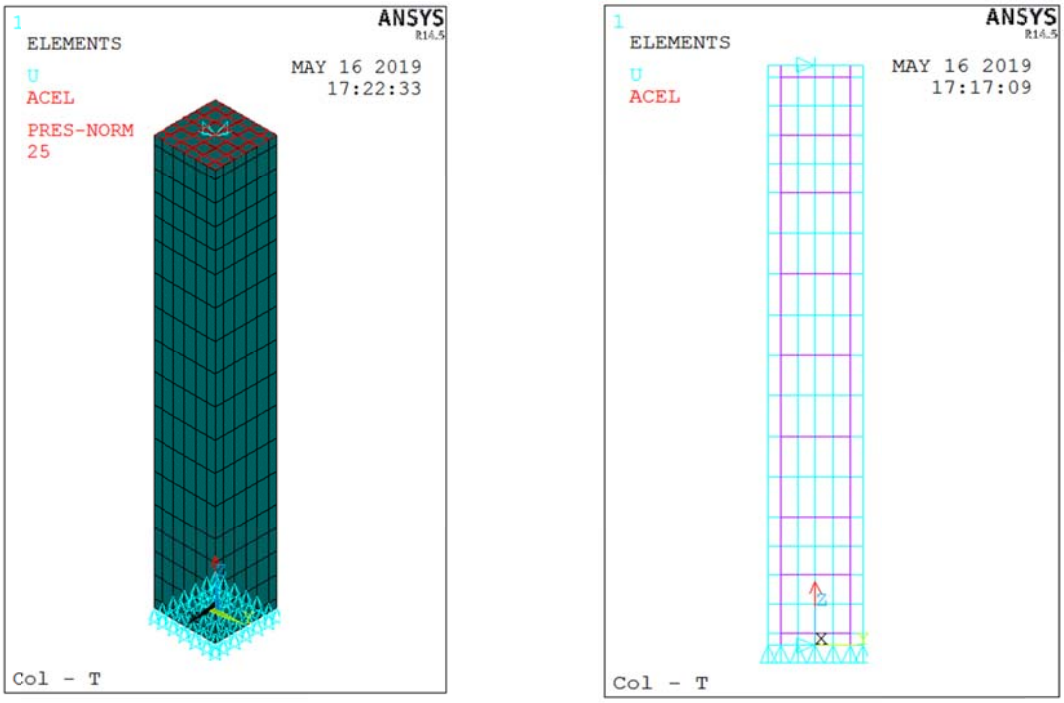

(a) Elements and boundary conditions (b) Longitudinal and transversal reinforcement

Fig. 15. Column model including concrete elements, reinforcement, boundary conditions and, applied surface pressure.

4.4 Applied Loads and Analysis Type

In the experimental test, two distinct loading conditions have been applied to the tested columns; the temperature load during heating and cooling processes and the axial load which has been applied using the hydraulic jack. To apply the temperature load, an additional degree of freedom "Temp" should be defined first to trigger the elements capabilities that relates to the temperature induced effects. The time-temperature relations; which are shown in Fig. 5, have been applied for each corresponding model. It is worth to mention that the furnace temperature has been applied to the outer surface of the outer elements which is in direct contact to the hot air inside the furnace while the elements which are located at the center core of the column have been subjected to the measured temperature. Furthermore, to apply the axial load, a surface pressure has been defined at the column's upper face to simulate the pressure created by the hydraulic jack.

To allow for applying the two loading conditions in the same way as in experimental conditions, a step-by-step full nonlinear transient analysis has been utilized. Both geometric and material nonlinearities have been considered in the analysis. The temperature load's time history has been applied with every load step represents

one minute on the time-temperature relation. Simultaneously, the surface pressure time history has been applied with a constant zero pressure during the heating and cooling processes to simulate the inside-furnace stage. After reaching the maximum time of the time-temperature relation, an additional time with additional load step has been provided to apply the surface pressure load on the column's upper face in order to simulate the axial load test. During this phase, the temperature value has been kept at the room temperature while the surface pressure has been increased gradually till the column's failure. A number of 100 sub-steps have been utilized during this time step.

4.5 Numerical Modeling Results

The full nonlinear transient analysis has been triggered for each model and the results have been obtained. The results include the body temperature distribution inside the column, the load-axial displacement behavior of the studied columns and, the ultimate axial capacity of the studied columns. To verify the modeling process, the obtained results have been compared to the experimental test results.

4.5.1 Body temperature distribution

For the first obtained result; which is the distribution of the body temperature across the column, a section located at the column's mid height has been selected to show the contours of the body temperature that the column has been affected by. Due to expected variation of the body temperature with respect to time, a snapshot has been taken every 50 minutes for the body temperature on the selected cross section. The obtained snapshots are shown in **Fig. 16**. According to this figure, at the beginning of heating, Time = 0.02 minute; all the elements have almost the same temperature which equals to the room temperature as shown in **Fig. 16 (a)**.

When the temperature has been increased during heating process of the furnace, the temperature of the outer faces of the outer rows of elements has reached the same temperature of the furnace; 399.874 ºC (Time = 50 minutes), while the temperature of the column's core elements reached much lower temperature of about 135ºC. For the intermediate elements between the outer rows and the column core elements, the temperature varies between the two temperature values of these elements. By further heating, the temperature of the outer faces has reached 400 ºC while that of the inner elements has increased gradually up to 260.045 ºC at time of 150 minutes. This means that the heat transfer flow has continued over time from the outer surface to the column's core which simulates the heating process. After the heating process has been stopped after the planned duration, the furnace door has been opened and the specimen has been allowed to cool off by to the room temperature. Accordingly, the temperature of the outer faces of the outer elements has started to decrease gradually. However, the temperature of the column's core elements has been noticed to increase. This may be due to the fact that just after heating stops, the heat transfer flow still in the same direction from the outer faces to the core resulting in increasing the temperature of the inner regions as shown in **Fig. 16 (e)**. When the cooling process has continued, the direction of the heat flow has inverted and the column's core has started to lose its temperature over the time. It can be noticed that the rate of losing the body temperature of the inner elements is less than that of the elements at the column surfaces which is expected due to their direct contact with the surrounding air which rapidly lost its temperature due to opening the furnace door. Finally, it is worth to mention that the temperature distribution is symmetric during the whole heating and cooling processes. Another sample of the temperature distribution across the column's cross section is shown in **Fig. 17**.

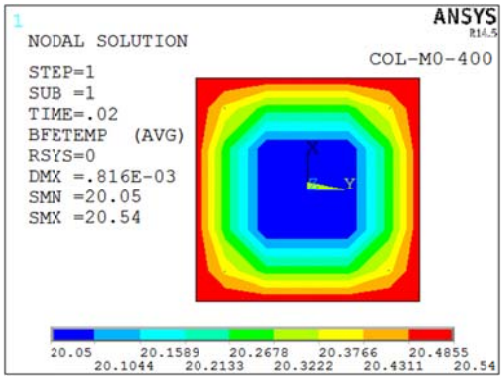

(a) Time = 0.02 Min.

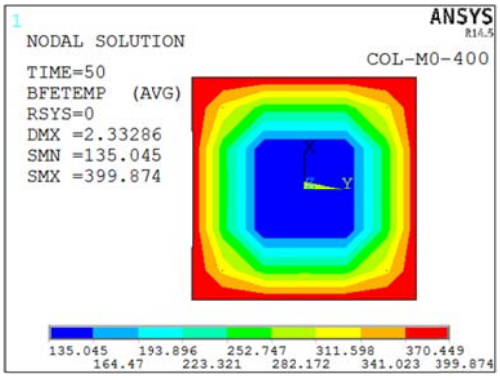

(b) Time = 50 Min.

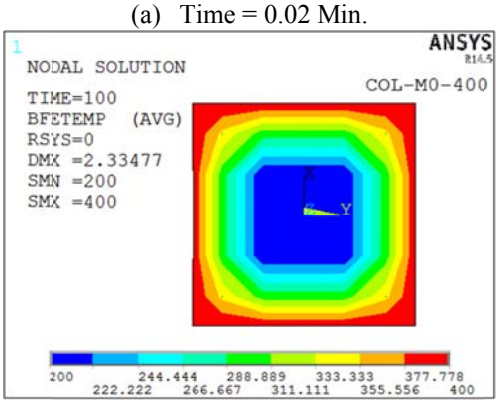

(c) Time = 100 Min.

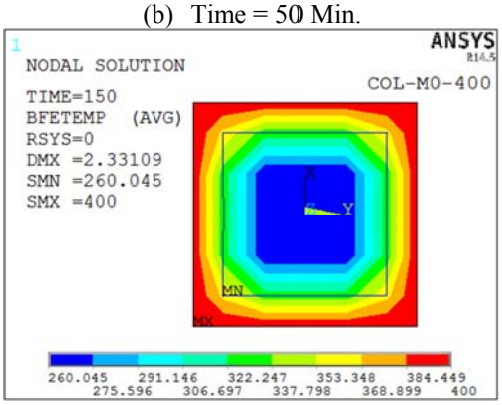

(d) Time = 150 Min.

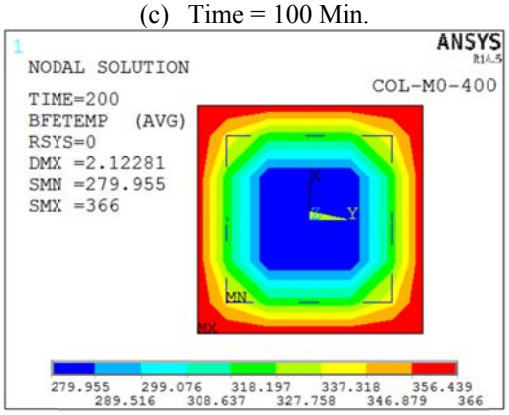

(e) Time = 200 Min.

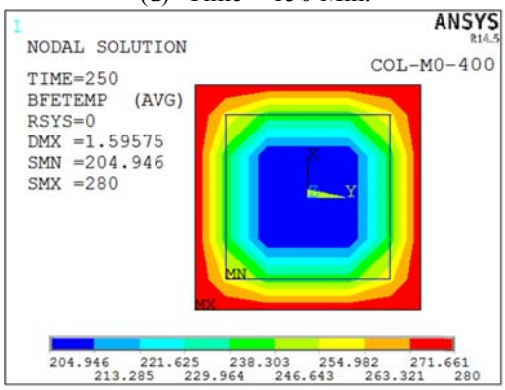

(f) Time = 250 Min.

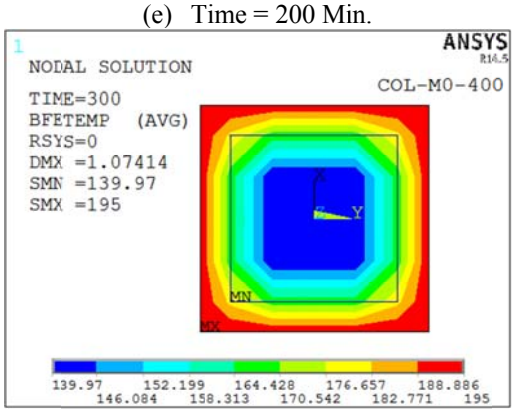

(g) Time = 300 Sec

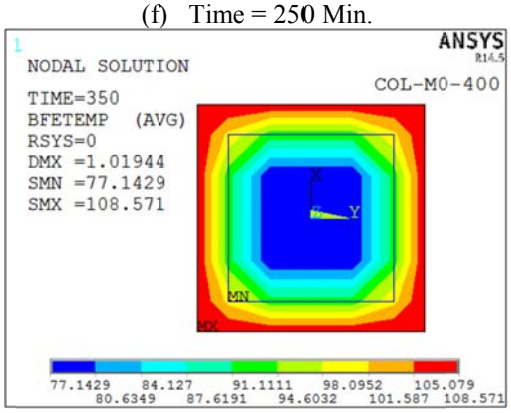

(h) Time = 350 Sec

Fig. 16. Temperature distribution on the cross section of specimen C-M0-400 at mid height.

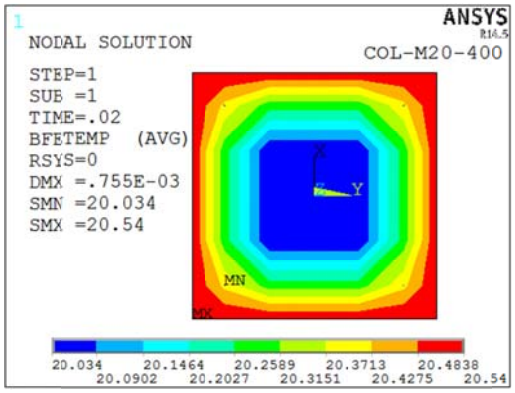

(a) Time = 0.02 Min.

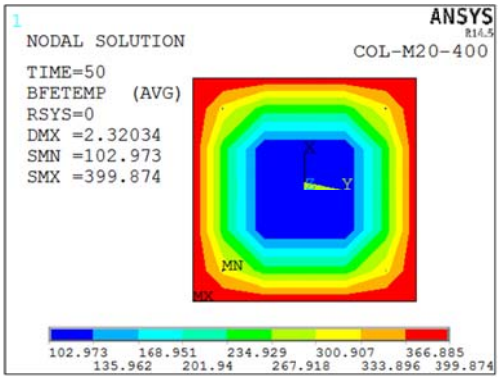

(b) Time = 50 Min.

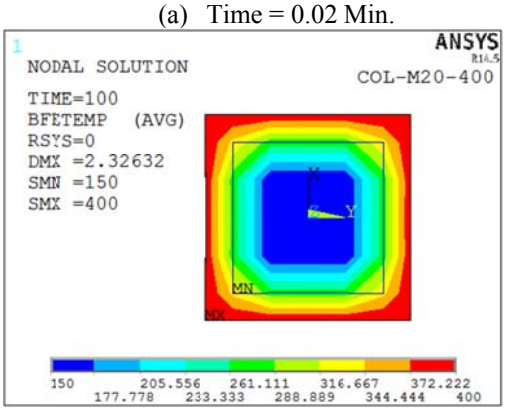

(c) Time = 100 Min.

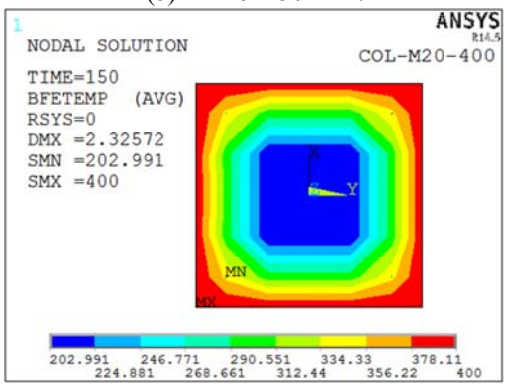

(d) Time = 150 Min.

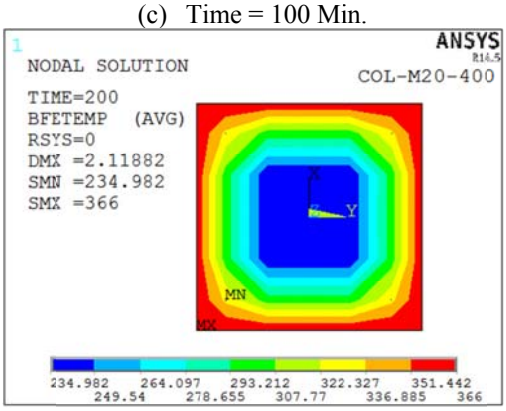

(e) Time = 200 Min.

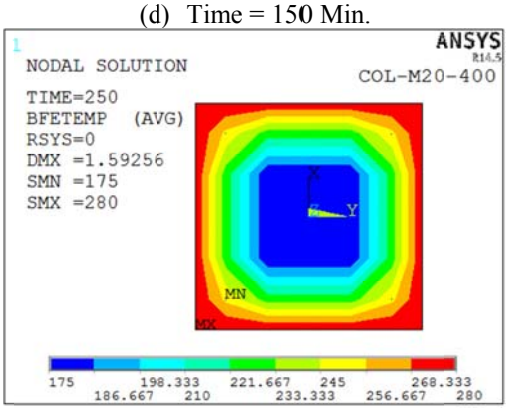

(f) Time = 250 Min.

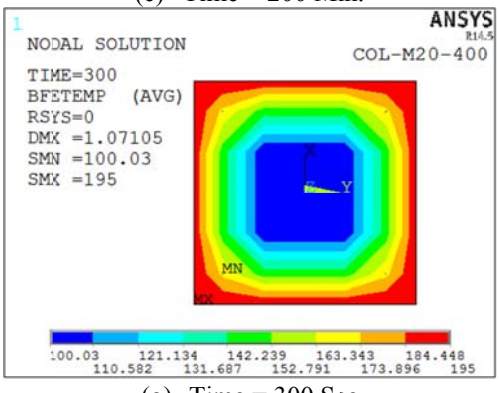

(g) Time = 300 Sec

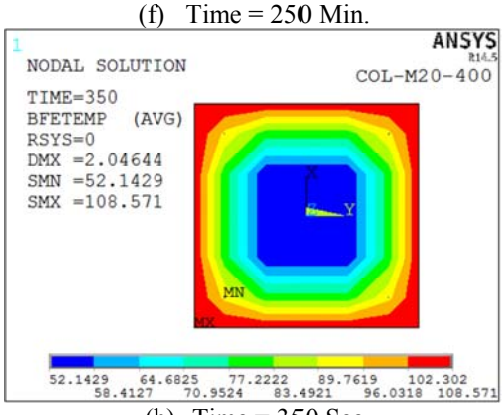

(h) Time = 350 Sec

Fig. 17. Temperature distribution on the cross section of specimen C-M20-400 at mid height.

4.5.2 Ultimate capacity and axial load-axial displacement behavior

The axial load-axial displacement relations for the nine studied columns have been obtained, plotted and, compared to those of the experimental tests. A comparison between the load-axial displacements relations of the columns of group [A] in which no elevated temperature has been applied to the columns are shown in **Fig. 18**. Similar comparisons have been constructed and are shown in **Fig. 19** and **Fig. 20** for groups [B] and [C]; respectively. A list of the obtained ultimate axial capacity from the FE models along with those obtained from the experimental program is listed in **Table 5**.

4.5.2.1 Group [A]

As can be noticed from **Fig. 18**, the FE models could successfully predict the ultimate capacity of the tested columns. However, there are some differences between the behaviors that have been obtained from the FE models and their corresponding experimental tests. This is may be due to the concave of the first part of the stress-strain curve of concrete in reality as schematically illustrated in **Fig. 21**. This concave part cannot be modeled in the used software; ANSYS, because it does not allow any stiffness to be greater than the initial stiffness of the stress-strain curve. Even if there will be stress stiffening, the stiffness in this case should be less than the initial tangent stiffness. Consequently, this difference between the modeled stress-strain relation and the actual one affects the load-axial displacement behavior especially at the early loading stages. However, this difference has not affected the obtained ultimate capacities of the FE models.

According to the FE results of the unheated specimens, it can be noticed that the difference between the FE and the experimental results ranges between 0.27% and 2.79% which means that the FE models can accurately predict the ultimate capacity of the tested columns. Furthermore, the specimen with 10% of its fine aggregate has been replaced by crumbed rubber shows lower failure load by about 4.5% comparing to the original case where its fine aggregate has not been replaced by any other material. Moreover, if the percentage of the replaced fine aggregate with the crumbed rubber is increased to 20%, the ultimate capacity decreases by about 12% comparing to the original case.

4.5.2.2 Group [B]

For specimens of group [B] which have been subjected to a temperature of 400ºC for three hours, **Fig. 19** shows a comparison between the obtained axial load-axial displacement behavior from the FE models with the experimental results of these specimens. As can be noticed from this comparison, the FE models have succeeded in predicting the ultimate axial load carrying capacity of these specimens. However, a difference in the behavior between the experimental test and the numerical model exists. This is similar to the difference between the experimental and numerical behaviors that has been highlighted before in the unheated specimens and it, possibly, owes to the same reason.

According to this figure, the difference between the ultimate capacities of the FE models and those of the experimental tests ranges between 0.5% and 4.59%. This small difference illustrates the good agreement between the ultimate capacity of the FE models and the experimental tests. Furthermore, as in the unheated columns, the existence of the crumbed rubber has decreased the ultimate capacity of the column by about 6% to 23% when replacing 10% and 20% of the fine aggregate with the crumbed rubber; respectively. This can be due to the decrease in the concrete strength when the crumbed rubber has replaced part of its fin aggregate. Another reason for this loss in capacity is that at elevated temperatures, the concrete itself loses a significant portion of its strength. That is why this group shows lower ultimate capacities comparing to the corresponding cases in the unheated case; group [A].

4.5.2.3 Group [C]

For the last group of specimens; group [C], which have been subjected to a higher temperature of 600ºC for the same duration as group [B]; three hours, **Fig. 20** shows a comparison between the obtained axial load-axial displacement behavior from the FE models with the experimental results of the specimens of group [C]. According to this comparison, the FE models have also succeeded in predicting the ultimate axial load carrying capacity of this group with a similar difference in the behavior between the experimental test and the numerical model exists as in the two previous groups. The percentage of difference in the ultimate capacities between the FE and the experimental results ranges between 0.52% and 1.32% which indicates the good agreement between the obtained FE and experimental ultimate capacities. Furthermore, using the concrete with the crumbed rubber has decreased the ultimate capacity by about 14% and 28% for 10% and 20% replacement of fine aggregate by the crumbed rubber; respectively.

Finally, **Table 5** shows a summary of the obtained FE results along with the experimental program results for comparison purposes. As can be noticed from this table, the maximum percentage of difference between FE results and experimental ones is about 6.6% for the axial displacement and 3.7% for the failure load; i.e. the ultimate axial capacity of the column. Also, it can be concluded that using the crumbed rubber

instead of a portion of the fine aggregate results in decreasing the ultimate capacity of the column. The percentage of loss in the ultimate capacity increases when the crumbed rubber percentage in the concrete increases.

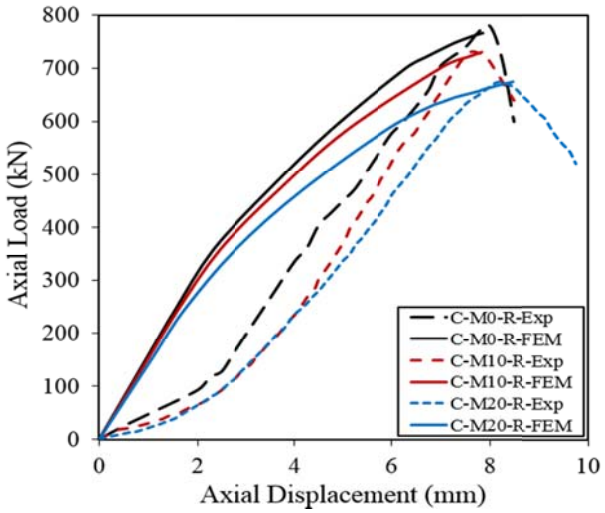

Fig. 18. Comparison between experimental and FEM results for group [A].

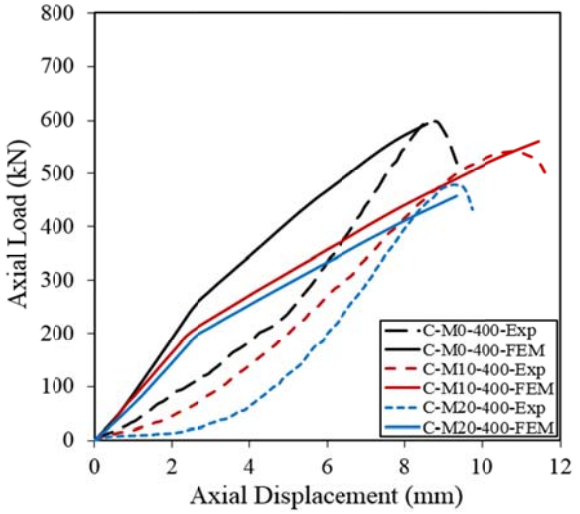

Fig. 19. Comparison between experimental and FEM results for group [B].

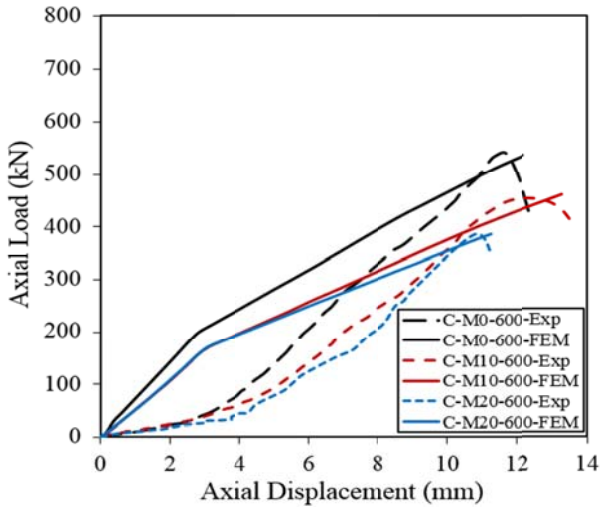

Fig. 20. Comparison between experimental and FEM results for group [C].

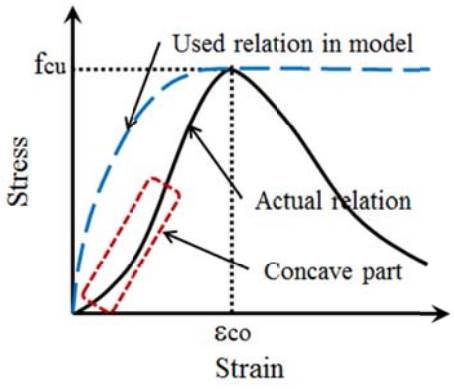

Fig. 21. Schematic representation for the actual and the modeled stress-strain relation of concrete.

Table 5: Summary of the numerical results

Specimen ID	Axial displacement (mm)			Ultimate load (kN)		
	Experimental	Numerical	Difference (%)	Experimental	Numerical	Difference (%)
C-M0-R	8.00	7.86	-1.70	788	766	-2.79
C-M10-R	7.75	7.84	1.22	733	731	0.27
C-M20-R	8.25	8.47	2.71	675	676	0.15
C-M0-400	8.75	8.59	-1.86	597	594	-0.50
C-M10-400	10.75	11.46	6.59	540	560	3.70
C-M20-400	9.25	9.36	1.17	479	457	-4.59
C-M0-600	11.75	12.16	3.53	540	535	-0.93
C-M10-600	12.50	13.27	6.18	455	461	1.32
C-M20-600	10.75	11.24	4.56	385	387	0.52

V. CONCLUSIONS

In this paper, an experimental program including nine square short columns with various crumb rubber content were carried out in order to investigate the effect of elevated temperatures on the behavior of short reinforced crumb rubber concrete columns. The nine columns were divided into three groups each of them contained three columns with different crumb rubber content. The crumb rubber content was utilized as a partial replacement of the fine aggregate of 0%, 10%, and 20% of the fine aggregate's volume. The first group was subjected to axial load testing at ambient room temperature without heating. The second and the third groups were heated first for three hours to a temperature of 400ºC and 600ºC for the second and the third group, respectively, and then left to cool down to room temperature and then were subjected to axial load test.

Furthermore, numerical models using the well-known FE software, ANSYS; were constructed to simulate these columns' behavior when subjected to elevated temperatures. The nonlinear material properties of the constituent materials were considered. Same sequence of heating, cooling and, axial loading of the columns was successfully simulated in the numerical models. These numerical models can be the basis for carrying out any further required parametric study in order to study the effect of any specific parameter on such columns.

Based on the results of both of the experimental and numerical investigations, the following conclusions can be drawn:

1. Using crumb rubber in concrete had a negative effect on its compressive strength, as the compressive strength values in case of crumb rubber concrete decreases with the increase of the quantity of crumb rubber.
2. Using waste tire rubber in concrete had an adverse influence on the load carrying capacity and stiffness of the heated and unheated columns. When the rubber content was increased from 10% to 20% for the unheated columns, the loss in the axial load carrying capacity was increased from about 7% to about14% and the percentage of loss in the secant stiffness was increased from about 4% to about 17% with respect to the control specimen (C-M0-R).
3. For both heated and unheated columns, the loss in their axial load capacity is lower than the loss in their secant stiffness. This may be due to the loss in their capacity which was accompanied; frequently, by an increase in their axial displacement.
4. The elevated temperature has a significant effect on the load carrying capacity of the columns without rubber. The axial load carrying capacity of the tested columns has lost about 24% and 31% of their capacities comparing to the un-heated one when the applied elevated temperature has reached 400ºC and 600ºC; respectively.
5. For the columns with 10% crumb rubber has been used, the loss in their capacities reached about 26% and 38% of the similar unheated column's capacity when heated up to 400ºC and 600ºC; respectively.
6. If the crumb rubber amount was 20% of the fine aggregate, heating the columns up to 400ºC and 600ºC results in increasing the percentage of the loss in their capacities to about 32% to 43% with respect to the unheated column containing the same amount of crumb rubber; respectively.
7. Exposing the columns with 0%, 10%, and 20% crumb rubber to elevated temperature 600^{o}C results in a significant loss of their stiffness by about 53%, 59%, and 63%; respectively.
8. For both heated and unheated columns, the loss in their axial load capacity is lower than the loss in their secant stiffness. This may be due to the loss in their capacity which has been accompanied, frequently; by an increase in their axial displacement.
9. Good agreement between the obtained ultimate axial capacities from the numerical models and those correspondences which were obtained from the experimental test.
10. The numerical models succeeded in simulating the effect of heating and cooling processes and the temperature transfer from the outer surface of the column to its inner core and vice versa.
11. The obtained axial load-axial displacement behavior from the models showed some with respect to that of the experimental test. This is may be due to the concave part that usually occurs in the first part of the actual stress-strain curve of concrete at early loading stages. This concave part cannot be modeled in the used software, because it does not allow any stiffness to be greater than the initial stiffness of the stress-strain curve. However, this difference vanishes at ultimate stage and the accuracy of the obtained axial capacity was assessed and was proven to be in good agreement with the experimental ones.

REFERENCES

[1]. Ako T., Onoduku U., Oke S., Essien B., Umar A., and Ahmend A., "Environmental effects of sand and gravel mining on land and soil in Luku, Minna, Niger State, North Central Nigeria", Journal of Geosciences and Geomatics. 2014; 2(2):42-49.

[2]. Wulandari P.S. and Tjandra D., "Use of crumb rubber as an additive in asphalt concrete mixture", Procedia engineering, 171, 2017, 1384–1389.

[3]. Kashani A., Ngo T.D., Mendis P., Black J.R., and Hajimohammadi A., "A sustainable application of recycled tyre crumbs as insulator in lightweight cellular concrete", Journal of Cleaner Production, 149, 2017, 925–935.

[4]. Topçu I. B., "The properties of rubberized concrete", Cement and Concrete Research, 25 (2), 1995, 304–310.

[5]. Topçu I.B and Demir A., "Durability of rubberized mortar and concrete", ASCE Journal of Materials in Civil Engineering, 19(2), 2007, 173–178.
[6]. Kelestemur O., "Utilization of waste vehicle tires in concrete and its effect on the corrosion behavior of reinforcing steels", International Journal of Minerals, Metallurgy, and Materials, 17 (3), 2010, 363–370.
[7]. Benli A., Karatas M., and Gurses E., "Effect of sea water and MgSO4 solution on the mechanical properties and durability of self-compacting mortars with fly ash/silica fume", Construction and Building Materials, 146, 2017, 464–474.
[8]. Bideci A., Ozturk H., Bideci O. S., "Fracture energy and mechanical characteristics of self-compacting concretes including waste bladder tire", Construction and Building Materials,149, 2017, 669–678.
[9]. Mehmet G. M., Guneyisi E., Hansu O., et al., "Influence of waste rubber utilization on the fracture and steel-concrete bond strength propertiesof concrete", Construction and Building Materials, 101, 2015, 1113–1121.
[10]. M. Aiello M. and Leuzzi F., "Waste tyre rubberized concrete: properties at fresh and hardened state", Waste Management, 30, 2010, 1696–1704.
[11]. Bisht K., Ramana P.V. "Evaluation of mechanical and durability properties of crumb rubber concrete", Construction and Building Materials, 155, 2017, 811–817.
[12]. Al-Tayeb M., Bakar B.H.A., Akil, H.M., and Ismail H., "Performance of rubberized and hybrid rubberized concrete structures under static and impact load conditions", Experimental Mechanics, 53 (3), 2013, 377–384.
[13]. Qiao D., Baoshan H., and Xiang Sh., "Rubber modified concrete improved by chemically active coating and silane coupling agent", Construction and Building Materials, 48, 2013, 116–123.
[14]. Liu H., Wang X., Jiao Y., and Sha T., "Experimental Investigation of the mechanical and Durability Properties of Crumb Rubber Concrete", Materials, 9, 2016, 1-12.
[15]. Atahan A.O., and Yücel A., "Crumb rubber in concrete: Static and dynamic evaluation", Construction and Building Materials, 36, 2012, 617–622.
[16]. Abendeh R., Ahmad H.S., and Hunaiti Y.M., "Experimental studies on the behavior of concrete-filled steel tubes incorporating crumb rubber", Constructional Steel Research, 122, 2016, 251–260.
[17]. Youssef O., Hassanli R., and Mills J.E., "Mechanical performance of FRP-confined and unconfined crumb rubber concrete containing high rubber content", Journal of Building Engineering, 11, 2017, 115–126.
[18]. Mendis A. S.M., Al-Deen S., and Ashraf M., "Flexural shear behaviour of reinforced Crumbed Rubber Concrete beam", Construction and Building Materials, 166, 2018, 779–791.
[19]. Guo Y.C., Zhang J., Chen G., and Xie Z., "Compressive behaviour of concrete structures incorporating recycled concrete aggregates, rubber crumb and reinforced with steel fibre, subjected to elevated temperatures", Journal of Cleaner Production, 72, 2014, 193-203.
[20]. Youssef O., El Gawady M., and Mills J.E., "Experimental Investigation of Crumb Rubber Concrete Columns under Seismic Loading", Structures, 3, 2015, 13–27.
[21]. Yang F., Feng W., Liu F., Jing L., Yuan B., and Chen D, "Experimental and numerical study of rubber concrete slabs with steel reinforcement under close-in blast loading", Construction and Building Materials, 198, 2019, 423–436
[22]. Li, L.J., Xie,W.F., Liu, F., Guo, Y.C., and Deng, J., "Fire performance of high-strength concrete reinforced with recycled rubber particles", Magazine of Concrete Research, 63, 2011, 187-195.
[23]. Guo Y.C., Zhang J., Chen G. and, Xie Z., "Compressive behaviour of concrete structures incorporating recycled concrete aggregates, rubber crumb and reinforced with steel fibre, subjected to elevated temperatures". Journal of Cleaner Production, 72, 2014, 193-203
[24]. Nenad S., Dragan P., Dragoslav S. and, Nemanja M., "New stress-strain model for concrete at high temperatures", Journal of Technical Gazette, 3, 2017, 863-868.
[25]. Zhong T., Xing-Qiang W. and, Brian U., "Stress-strain curves of structural steel and reinforcing steel after exposure to elevated temperatures", Journal of Materials in Civil Engineering, 9, 2013, 1306-1316.
[26]. Viktor G., Darius B., and, Gintaris K., "Numerical simulation strategy of reinforced concrete tunnel bearing members in fire", The Baltic Journal of Roads and Bridge Engineering, 1, 2006, 6-9.

Mohamed S. Gomaa" Behavior of Short Reinforced Crumb Rubber Concrete Columns Subjected to Elevated Temperatures" International Journal of Engineering Science Invention (IJESI), Vol. 08, No. 05, 2019, PP 11-27